Spatial regulation of actin dynamics: a tropomyosin-free, actin-rich compartment at the leading edge

Vera DesMarais[1,*], Ilia Ichetovkin[1], John Condeelis[1] and Sarah E. Hitchcock-DeGregori[2]

[1]Department of Anatomy and Structural Biology, Albert Einstein College of Medicine,1300 Morris Park Avenue, Bronx, NY 10461, USA
[2]Department of Neuroscience and Cell Biology, UMDNJ-Robert Wood Johnson Medical School, 675 Hoes Lane, Piscataway, NJ 08854, USA
*Author for correspondence (e-mail: vogniew@aecom.yu.edu)

Accepted 4 September 2002
Journal of Cell Science 115, 4649-4660 © 2002 The Company of Biologists Ltd
doi:10.1242/jcs.00147

Summary

Rapid polymerization of a network of short, branched actin filaments takes place at the leading edge of migrating cells, a compartment enriched in activators of actin polymerization such as the Arp2/3 complex and cofilin. Actin filaments elsewhere in the cell are long and unbranched. Results reported here show that the presence or absence of tropomyosin in these different actin-containing regions helps establish functionally distinct actin-containing compartments in the cell.

Tropomyosin, an inhibitor of the Arp2/3 complex and cofilin function, was localized in relation to actin filaments, the Arp2/3 complex, and free barbed ends of actin filaments in MTLn3 cells, which rapidly extend flat lamellipodia following EGF stimulation. All tropomyosin isoforms examined using indirect immunofluorescence were relatively absent from the dynamic leading edge compartment, but did colocalize with actin structures deeper in the lamellipodium and in stress fibers. An in vitro light microscopy assay revealed that tropomyosin protects actin filaments from cofilin severing. The results suggest that tropomyosin-free actin filaments under the membrane can participate in rapid, dynamic processes that depend on interactions between the activities of the Arp2/3 complex and ADF/cofilin that tropomyosin inhibits elsewhere in the cell.

Key words: Actin, Arp2/3 complex, Tropomyosin, Cofilin, Cytoskeleton

Introduction

In response to a variety of extracellular stimuli, actin filament assembly at the leading edge of motile cells causes protrusion during cell crawling and chemotaxis, nerve growth and cell spreading (Lauffenburger and Horwitz, 1996). The actin filament network immediately under the plasma membrane in regions of rapid cellular protrusion consists of short, branched filaments while those deeper in the cortex, as well as at focal adhesions, stress fibers and in microvilli, are much longer and rarely branched (Bailly et al., 1999; Small et al., 1995; Small et al., 2002; Svitkina and Borisy, 1999). The formation of the branched network is postulated to involve nucleation of new filaments by activated Arp2/3 complex (Blanchoin et al., 2000a; Mullins et al., 1998) (reviewed in Borisy and Svitkina, 2000; Condeelis, 2001; Pollard et al., 2000). Models have been presented in which activated Arp2/3 complex generates branches and ADF/cofilin (hereafter called cofilin) enhances filament turnover and nucleation activity of the Arp2/3 complex (reviewed in Borisy and Svitkina, 2000; Condeelis, 2001; Ichetovkin et al., 2002; Pollard et al., 2000). Support for the models comes from studies showing that the Arp2/3 complex and cofilin are localized in the network of branched filaments at the leading edge (Bailly et al., 1999; Chan et al., 2000; Svitkina and Borisy, 1999).

The formation of the branched network in the leading edge domain of the actin cytoskeleton is spatially and temporally regulated using both positive and negative mechanisms. For example, the Arp2/3 complex is localized in the leading edge (Bailly et al., 1999; Svitkina and Borisy, 1999), where it is activated by membrane bound factors, Rho-family GTPases and PIP_2, which in turn activate cellular WASp/Scar proteins that bind to the Arp2/3 complex (reviewed in Borisy and Svitkina, 2000; Higgs and Pollard, 2001; Small et al., 2002). In addition, actin filaments serve as obligate secondary activators of the Arp2/3 complex activity (Ichetovkin et al., 2002). Cortactin stabilizes branches (Uruno et al., 2001; Weaver et al., 2001). Cofilin, required for the formation of barbed ends at the leading edge (Zebda et al., 2000), severs actin filaments, thereby increasing the number of free barbed ends, polymerization, and the number of ATP-containing filaments leading to enhanced Arp2/3 complex activation (Ichetovkin et al., 2002). Cofilin also ensures a supply of actin monomers for polymerization and the turnover of the Arp2/3 complex by severing and increasing the off-rate of actin monomers from the pointed end (reviewed by Bamburg, 1999; Carlier et al., 1997; Hawkins et al., 1993; Condeelis, 2001). Experiments using the actin drug jasplakinolide showed that protrusion of lamellipodia in migrating chick fibroblasts is tightly coupled to actin filament disassembly, suggesting that ongoing actin filament assembly is facilitated by free actin monomers derived from filament disassembly (Cramer, 1999). Tropomodulin, a protein that together with tropomyosin inhibits association and dissociation of actin monomers from the pointed end of actin filaments (Weber et al., 1994; Weber et al., 1999), may also favor barbed end incorporation of actin monomers.

Some factors negatively regulate formation of the branched actin filament network. ATP hydrolysis and phosphate dissociation following actin polymerization promote

dissociation of filament branches (Blanchoin et al., 2000b). Phosphorylation of cofilin inhibits its severing and depolymerizing activities (Agnew et al., 1995; Blanchoin et al., 2000c; Moriyama et al., 1996; Ressad et al., 1998). Tropomyosin, a protein that binds along the sides of actin filaments, inhibits nucleation and branch formation by the Arp2/3 complex (Blanchoin et al., 2001) and cofilin-F-actin interaction in vitro (Bernstein and Bamburg, 1982; Nishida et al., 1985; Ono and Ono, 2002). Proteins that cross-link actin into stable structures, such as α-actinin, fascin and fimbrin, may also protect actin filaments against branching and severing.

The molecular models put forward to date to explain the processes that take place at the leading edge of motile cells primarily depend on in vitro experiments with the Arp2/3 complex. Identification of multiple domains of the actin cytoskeleton within cells and how they relate to the Arp2/3 complex localization and function at the leading edge requires spatial and temporal analysis in a well-defined cell model. The extent to which cofilin and the Arp2/3 complex contribute to lamellipodium extension has been studied in MTLn3 cells following EGF stimulation. Barbed ends at the leading edge are generated by cofilin during EGF stimulation (Zebda et al., 2000). Cofilin severing is required for both barbed end generation and protrusion of the leading edge (Chan et al., 2000). Also, the branching activity of the Arp2/3 complex is required for lamellipodium protrusion during EGF stimulation (Bailly et al., 2001).

Our goal in the present study was to relate cellular compartments in which the Arp2/3 complex and cofilin-mediated actin polymerization occurs to the localization of tropomyosin. Our hypothesis was that since these activities are inhibited by tropomyosin, tropomyosin would be excluded from the leading edge of actively protruding cells. Although the tropomyosin localization has been reported in numerous cell types (reviewed in Lin et al., 1997), its location in relation to the dendritic actin network has not been investigated. Here we relate the biochemical effects of tropomyosin on the activities of the Arp2/3 complex and cofilin to the cellular localization of tropomyosins with respect to the Arp2/3 complex, barbed ends, and F-actin at the leading edge during rapid lamellipodium extension. We used an optically flat cell (MTLn3) with well-defined kinetics of EGF-stimulated protrusion that allows cellular localization of proteins at the leading edge at high resolution. Our results indicate that tropomyosin plays a regulatory role to confine the activities of the Arp2/3 complex and cofilin to the leading edge.

Materials and Methods

Cell culture

MTLn3 cells were cultured in α-MEM (Gibco Laboratories) with 5% FCS, as previously described (Bailly et al., 1998a; Segall et al., 1996). Cells were plated at low density in complete medium for 24 hours. Before the experiment, cells were starved for 3 hours in α-MEM medium containing 0.35% BSA (starvation medium). For stimulation, cells were treated for 50 seconds or 3 minutes with a final concentration of 5 nM murine epidermal growth factor (EGF; Life Technologies) in starvation medium.

Primary antibodies

Previously characterized mouse monoclonal and rabbit polyclonal antibodies against tropomyosin were generously supplied by colleagues, or purchased. Six different antibodies were screened that together recognize tropomyosins expressed by all four tropomyosin genes representing most, if not all, the isoforms in MTLn3 cells. Of these, two (LC24 and αf9d) were selected for more extensive analysis based on their staining characteristics and ability to detect a wide range of tropomyosin isoforms.

LC24 is a mouse monoclonal (IgG), provided by Jim Lin (University of Iowa). It is specific to TM4, a short TM encoded by the *TM4* gene [*δ-TM* (Lin et al., 1985a; Lin et al., 1988)]. It was prepared against human protein, but it also recognizes mouse protein.

αf9d is a rabbit polyclonal, provided by Peter Gunning (University of Sydney). It recognizes the C-terminal region of α- and β-TM isoforms expressing exon 9d (Schevzov et al., 1997). In mouse it crossreacts with a number of short and long TM isoforms: αTM2, αTM3, βTM1, βTM6 (all long TM isoforms), and αTM5a and αTM5b, and homologous short β-TM isoforms.

CG3 is a mouse monoclonal (IgM), provided by Jim Lin (University of Iowa). It cross reacts with the exon 1b-encoded N-terminus of products of the *TM5* gene (*γ-TM*), short, non-muscle tropomyosins (Lin et al., 1985a; Lin et al., 1988; Vera et al., 2000). It was prepared against human immunogens, but also recognizes mouse proteins.

IV15 is a mouse monoclonal (IgM) provided by Fumio Matsumura (Rutgers University) with a wide specificity [F. Matsumura, personal communication (Matsumura et al., 1983)].

CGβ6 is a mouse monoclonal (IgM) provided by Jim Lin (University of Iowa) that crossreacts with TM2 and TM3, long α-TM isoforms (Lin et al., 1985a; Lin et al., 1988) that are also recognized by αf9d and TM311.

TM311, a mouse monoclonal IgG purchased from Sigma, crossreacts with the N-terminus of long α and β-TM isoforms (Nicholson-Flynn et al., 1996).

Anti-p34 (AE360) is a rabbit IgG generated using a peptide immunogen of a sequence of the p34 protein in the Arp2/3 complex (Bailly et al., 2001).

It is unlikely that the lack of binding of anti-TM at the leading edge is a consequence of non-linear binding of antibody at low concentration of antigen, since both monoclonal (e.g. CG3) and polyclonal (e.g. αf9d) antibodies gave the same tropomyosin distribution as far as absence of labeling of the leading edge is concerned, even though they generally exhibit different binding curves.

Immunofluorescence

Cells were plated on glass-bottom dishes (MatTek Corporation) as previously described (Bailly et al., 1998a) and left untreated or stimulated with EGF. They were fixed with 3.7% formaldehyde in cytoskeletal buffer (5 mM KCl, 137 mM NaCl, 4 mM $NaHCO_3$, 0.4 mM KH_2PO_4, 2 mM $MgCl_2$, 5 mM Pipes, 2 mM EGTA, 5.5 mM glucose, pH 6.1 (Small et al., 1978), at 37°C for 5 minutes. Cells were permeabilized at room temperature for 20 minutes with 0.5% Triton X-100 in cytoskeletal buffer. They were rinsed once and then incubated in 0.1 M glycine (in cytoskeletal buffer). After five washes with TBS (20 mM Tris, 154 mM NaCl, pH 8), cells were blocked/stabilized in TBS with 1% BSA, 1% FCS, and 5 μM phalloidin (Calbiochem-Novabiochem) for 20 minutes. For F-actin staining, phalloidin was supplemented with 0.5 μM rhodamine phalloidin (Molecular Probes). This was followed by incubation with primary antibody at room temperature for one hour. Cells were rinsed five times for five minutes with TBS containing 1% BSA and incubated with secondary antibody, goat anti-rabbit fluorescein-conjugated IgG (ICN Biomedicals), or Cy5 conjugated donkey anti-mouse IgG (Jackson ImmunoResearch), for one hour at room temperature. After five final washes with TBS (containing 1% BSA), cells were mounted in 50% glycerol in TBS, supplemented with 6 mg/ml N-propyl gallate and 0.02% sodium azide.

Visualization of free barbed ends

For double labeling of actin nucleation sites (barbed ends) and tropomyosin (αf9d), a previously described protocol was used (Bailly et al., 1999; Chan et al., 1998). Briefly, cells were stimulated with EGF for 50 seconds or 3 minutes, immediately followed by permeabilization with cytoskeletal buffer, containing 0.45 μM of biotin-labeled G-actin (Cytoskeleton), 1% BSA, and 0.025% saponin. The distribution of biotin-actin was identified using a Cy5-coupled anti-biotin antibody (Jackson ImmunoResearch). Tropomyosin was visualized by incubating cells with antibody αf9d for 1 hour, followed by incubation with a goat anti-rabbit fluorescein-conjugated IgG (ICN Biomedicals).

Microscopy and fluorescence quantification

All images were taken on an Olympus IX70 microscope using constant settings with 60× NA 1.4 infinity-corrected optics coupled to a computer-driven cooled CCD camera using IP lab spectrum software (VayTek). Images were captured below the saturation level of the camera. For the fluorescence quantification, all digitized images were linearly converted in NIH Image (program developed by the National Institute of Health, available on the internet at http://rsb.info.nih.gov/nih-image) and analyzed using different macros. For double-labeling measurements (Fig. 5) cell perimeters were traced by fluorescence threshold in the non-tropomyosin channel and also applied to the tropomyosin channel. The measurements were taken on lamellipodia, avoiding regions of cells that did not contain lamellipodia. The software macro automated the collection of pixel intensity in a perimeter of the cell starting 1.98 μm outside the cell and extending 4.18 μm into the cell in 0.22 μm steps. Lamellipodia are flat and of uniform thickness, so there is negligible contribution of the variation of thickness to the fluorescence intensity (Bailly et al., 1998a; Bailly et al., 1998b; Chan et al., 1998; Rotsch et al., 2001). This procedure included subtraction of background fluorescence from the measured cellular fluorescence. The dark current noise of the camera is below the level of background fluorescence. Any signal measured above the dark current noise of the camera is in the linear range of the camera, up to saturation levels. In the conditions used, any signal above zero in the graph is in the linear range of the camera and above dark current noise levels. For a description of the system see http://www.aecom.yu.edu/aif.

For the determination of percent of a protein in a cell region, cell perimeters were traced by fluorescence threshold in the non-tropomyosin channel and also applied in the tropomyosin channel. Only cells were selected that were nearly perfectly surrounded by lamellipodia, without substantial regions where stress fibers contacted the cell membrane. For each region of the cell, fifteen cells were analyzed that had been stimulated with EGF for 3 minutes. Fluorescence intensities were measured using a software macro that automated the collection of pixel intensity in a perimeter of the cell that started at the cell membrane and extended into the cell in two steps, each of 0.88 μm width. The first 0.88 μm step is defined as the leading edge compartment, and the second 0.88 μm step is defined as the base of the lamellipodium. In addition, the fluorescence intensity of the whole cell was measured to allow percentage calculations at the leading edge and in the base of lamellipodia. To measure the percentage of actin and tropomyosin in stress fibers, a software macro was used that selects the region of the cell that contains stress fibers by fluorescence threshold in the actin channel and applies the same area to the tropomyosin channel.

Tropomyosin extraction experiments

To estimate the percent of the total tropomyosin that was free, not associated with the actin cytoskeleton, we used two independent experimental methods. In the first gel-based method, 100 mm plates of confluent MTLn3 cells were washed with phosphate buffered saline and permeabilized for one to four minutes with: 138 mM KCl, 10 mM Pipes, pH 7, 0.1 mM ATP, 3 mM EGTA, 4 mM $MgCl_2$, 0.025% saponin, 0.5% Sigma protease cocktail. To estimate total tropomyosin, in parallel, cells on plates were washed and lysed in 10 mM TrisHCl, pH 8.0, 10 mM EGTA, 0.025% saponin, 0.5% of a Sigma protease cocktail, for 10 minutes on ice to obtain the total cytoskeletal protein, and removed from the plates by scraping. NaCl was added to the samples to a final concentration of 0.2-0.5 M, and the samples were heated for 2 minutes at 100%. Following centrifugation for 10 minutes in a microfuge at 4°C, the supernatants containing tropomyosin, and other heat-stable proteins, were lyophilized. The samples were resuspended in the same volume of sample buffer and analyzed by SDS PAGE on 12% gels stained with Coomassie Blue.

The tropomyosin in the heat stable fraction was quantified by densitometry of the stained gels using a Molecular Dynamics model 300A computing densitometer. The tropomyosin region of the gel was identified by immunoblots using specific tropomyosin antibodies and tropomyosin standards. In the absence of permeabilization and lysis buffers there was no staining in the tropomyosin region of the gel. With the permeabilization procedure, 15±4% (n=5) of the total tropomyosin was removed.

In the second method based on immunofluorescence, a monolayer of EGF stimulated cells were fixed with formaldehyde and stained with LC24 as described in 'Immunofluorescence'. Another monolayer of EGF-stimulated cells was permeabilized with saponin, fixed with formaldehyde and stained with LC24 as described in 'Visualization of barbed ends'. Digital images of cells were taken at 20× magnification and pixel intensities of the cell were measured using the NIH Image software as described in 'Microscopy and fluorescence quantification'. Cells extracted with saponin and then fixed with formaldehyde showed an 18% loss of fluorescence intensity presumably reflecting extraction of free tropomyosin not bound to actin filaments.

Protein purification

Actin was purified from rabbit skeletal muscle acetone powder (Spudich and Watt, 1971). Recombinant rat TM5a, a short non-muscle TM product of the *α-TM* gene, was cloned and expressed in *E. coli*, and purified as previously described (Moraczewska et al., 1999). Recombinant cofilin was expressed in *E. coli* and purified as previously described (Bamburg et al., 1991) with modifications as stated in Ichetovkin et al. (Ichetovkin et al., 2000).

Light microscopy severing assay

This severing assay has been described in detail and validated previously (Chan et al., 2000; Ichetovkin et al., 2002; Ichetovkin et al., 2000). Briefly, 10 μM recombinant rat TM5a in perfusion buffer (20 mM Pipes pH 7.0, 2 mM $MgCl_2$, 5 mM EGTA, 50 mM KCl, 1 mM ATP, 1 mM dithiothreitol) was reduced by heating to 58°C for 2 minutes, cooled to room temperature and kept on ice for the duration of the experiments. Chambers with pre-bound actin filaments (Ichetovkin et al., 2002) were perfused for 45 minutes with either 10 μM TM5a or perfusion buffer as a control. After 45 minutes, chambers were placed on a CCD-equipped inverted microscope (Olympus IX70), and unbound TM5a was washed away with anti-bleaching wash buffer (20 mM Pipes pH 7.0, 2 mM $MgCl_2$, 5 mM EGTA, 50 mM KCl, 1 mM ATP, 100 mM DTT, 5 mg/ml BSA, 6 mg/ml glucose, 0.2 mg/ml glucose oxidase, 0.036 mg/ml catalase), '0 second' time point rhodamine-fluorescent images were collected (with the 60× objective). Chambers were perfused under the microscope with 100 nM recombinant rat cofilin in 10 mM Tris pH 7.5, 100 mM DTT, 5 mg/ml BSA, 6 mg/ml glucose, 0.2 mg/ml glucose oxidase, 0.036 mg/ml catalase. After 1 minute of incubation with cofilin, images of the same field were taken. Images were quantified using NIH Image by counting number of filaments using

automatic thresholding. An increase in the total number of filaments in the same field indicated cofilin-severing activity. To avoid counting false breaks in the filament due to non-continuous labeling, thresholding levels were set to score only gaps between filaments larger than 0.3-0.4 mm. That led to the underscoring of small gaps even though they were clearly visible by eye (nearly all breaks formed after an initial 30 seconds), but resulted in much more consistent and reproducible quantitative data.

Results

In the present study we examined the cellular localization of tropomyosin, a negative regulator of the Arp2/3 complex (Blanchoin et al., 2001), in resting and stimulated cells in relation to F-actin, the Arp2/3 complex, and actin filament barbed ends. We used a line of metastatic rat mammary adenocarcinoma (MTLn3) cells (Segall et al., 1996) because it has proven to be an excellent model system for defining the functional domains of the actin cytoskeleton and for establishing the early steps in actin reorganization after stimulated protrusion. MTLn3 cells extend broad, flat lamellipodia in a well-defined series of steps after EGF stimulation (Bailly et al., 1998a; Chan et al., 1998; Segall et al., 1996). These lamellipodia are planar protrusion structures with a uniform thickness of 400-600 nm (Rotsch et al., 2001), making them ideal for the measurement of the location and amount of actin-associated proteins with high resolution. During EGF stimulation, the leading edge of MTLn3 cells does not contain ruffles (Rotsch et al., 2001), which are raised, non-planar regions of lamellipodia.

EGF-stimulated lamellipodium extension in MTLn3 cells depends on actin polymerization and results in a transient increase in the number of free barbed and pointed ends of filaments accompanied by the formation of a branched filament network in a narrow zone at the extreme leading edge (Bailly et al., 1999; Chan et al., 2000). This zone is enriched in the Arp2/3 complex and cofilin, proteins required for lamellipodium extension (Bailly et al., 2001; Bailly et al., 1999; Chan et al., 2000; Zebda et al., 2000).

In order to determine the general localization of tropomyosin in MTLn3 cells we used a broad spectrum of antibodies that recognize tropomyosin isoforms encoded by all four tropomyosin genes (α, β, γ, δ), and all tropomyosin types expressed in the cell (see Materials and Methods). The tropomyosin isoforms expressed in MTLn3 cells were evaluated using immunoblots of total cell extracts from unstimulated cells (Fig. 1). Antibody αf9d crossreacted with at least three major bands and additional minor bands, both long and short tropomyosins, some of which were identified using the TM311 and CGβ6 antibodies. These represent tropomyosins TM1/TM6 (not separated in this blot), TM2, TM3 and possibly small amounts of short isoforms. Two short isoforms encoded by the α-*TM* gene, TM5a and TM5b, were not detected using another antibody specific for these isoforms. The CG3 antibody crossreacted with one major band that consists of up to 11 isoforms of the γ-*TM* gene (TM5nm tropomyosins). The antibody LC24 crossreacted with a single band indicating that TM4, the only non-muscle isoform encoded by the γ-*TM* gene, is expressed well in MTLn3 cells. In summary, the major tropomyosin isoforms expressed in MTLn3 cells are the long isoforms TM1/TM6, TM2, TM3 and the short isoforms TM4 and one or more TM5nm.

The distribution of tropomyosin and F-actin during lamellipodium extension

Previous studies using these antibodies have shown the presence of multiple microfilament compartments within cells (Lin et al., 1985a; Lin et al., 1985b; Lin et al., 1988; Nicholson-Flynn et al., 1996; Percival et al., 2000). However, from these studies it is unclear whether tropomyosin is present in the leading edge of protruding lamellipodia [defined as the first 0.9 μm next to the membrane (Chan et al., 2000)]. This is the case either because the cell types studied had no distinct, protruding leading edge, or the history of the cell protrusion was not followed, or the staining was not related to the cell edge by phase contrast images or double labeling with markers for the leading edge. We examined cells stained with αf9d, LC24, CG3, CGβ6, TM311, and IV15 antibodies, which recognize tropomyosins encoded by all four tropomyosin genes, as discussed above. The results using all the antibodies were the same in that none stained the leading edge of protruding lamellipodia, although they stained other actin-containing structures to differing extents. Since the tropomyosin isoforms recognized by TM311 and CGβ6 were also recognized by αf9d, we did not proceed with a detailed cellular analysis using these antibodies. Illustrative results using the antibodies αf9d, LC24, CG3 and IV15 are shown in Figs 2-4. The antibodies LC24 and αf9d were selected for more extensive analysis because they stained actin structures well, including the base of lamellipodia close to the leading edge. All other antibodies mainly stained structures toward the middle of the cell, such as stress fibers. In addition, αf9d and LC24 recognized bands in immunoblots of MTLn3 cell extracts that are encoded by different tropomyosin genes (Fig. 1). The results of this analysis are shown in Fig. 5.

MTLn3 cells double-labeled for F-actin (rhodamine-phalloidin, Fig. 2A,E,I) and tropomyosin (LC24, Fig. 2B,F,J)

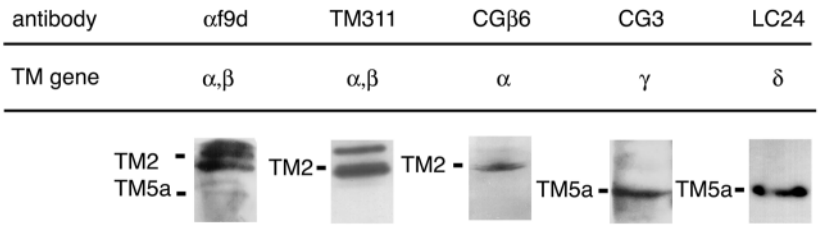

Fig. 1. Immunoblots of extracts of unstimulated MTLn3 cells with antibodies against tropomyosin. The positions of TM2 and TM5a standards in relation to the bands of the blots are indicated. The αf9d antibody recognizes long and short tropomyosin isoforms encoded by the *αTM* and *βTM* genes. These include, from top to bottom, TM1 and TM6 (not distinguishable on this blot), TM2, TM3, and minor amounts of short isoforms. The TM311 antibody shows the presence of at least three high molecular weight isoforms: TM1/6, TM2 and TM3. The CGβ6 antibody identifies the two faster migrating major forms seen in the αf9d and TM311 blots as TM2 and TM3. The blots using LC24 and CG3 recognize the major short tropomyosins expressed in MTLn3 cells as TM4 and one or more products of the *γTM* gene.

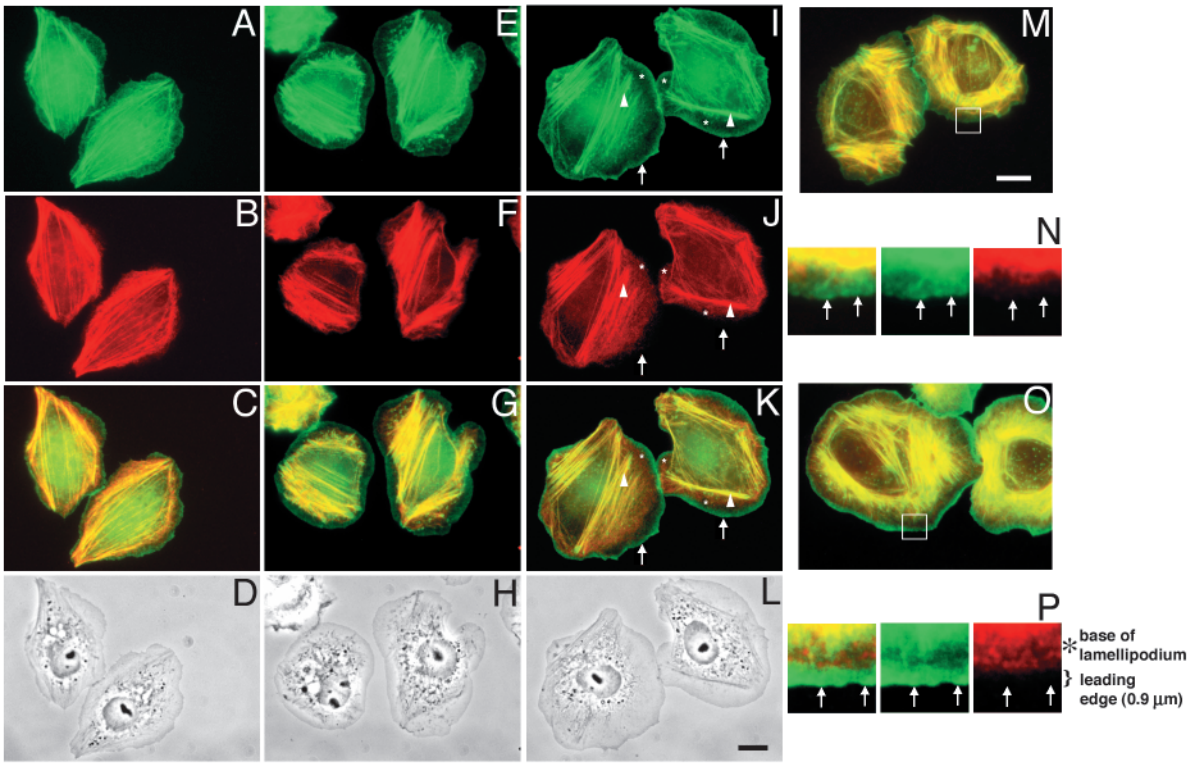

Fig. 2. Tropomyosin is absent from regions of the leading edge that contain a dense F-actin network. Cells were either unstimulated (A-D,M), or stimulated with EGF for 50 seconds (E-H) or 3 minutes (I-L,O). Phalloidin-stained F-actin is shown in panels A, E, and I and tropomyosin (antibody LC24) in panels B, F, and J. Double-labeling overlays are shown (C,G,K; green, F-actin; red, tropomyosin), as well as phase contrast images (D,H,L). Panel M shows double-labeling of unstimulated cells and panel O shows double labeling of cells stimulated with EGF for 3 minutes. In panels M and O, the white square indicates an area that is shown at higher magnification in the panels below (panel N and P, from left to right: double labeling, F-actin, tropomyosin). The size of the square is 6 μm by 6 μm. The scale bar in panel L indicates 10 μm and applies to panels A-L. The scale bar in panel M also indicates 10 μm and applies to panels M and O. Arrows indicate regions at the leading edge that show F-actin staining but no tropomyosin. Arrowheads indicate labeling of actin stress fibers by both rhodamine-phalloidin and LC24 (tropomyosin). The diffuse, non-stress fiber actin network in the base of the lamellipodium is indicated by an asterisk and contains both F-actin and tropomyosin.

showed bright F-actin staining at the leading edge before (Fig. 2A-D,M,N) and after (Fig. 2E-L,O,P) EGF stimulation, reflecting the newly polymerized F-actin network adjacent to the plasma membrane that is generated during lamellipodium extension. However, tropomyosin was absent from this dynamic leading edge compartment, although there was substantial overlap of F-actin and tropomyosin staining in the rest of the cell (overlays, Fig. 2C,G,K,M-P), especially in stress fibers and the diffuse non-stress fiber actin network in the base of the lamellipodium (indicated by an asterisk). Higher magnification images of the boxed regions of the cells in Fig. 2M,O show that in both unstimulated cells (Fig. 2N) and EGF-stimulated cells (Fig. 2P) tropomyosin (red) was absent from the dynamic leading edge compartment whereas F-actin (green) was present up to the cell membrane, and thickens after stimulation. However, both tropomyosin and F-actin were present just beyond the dynamic leading edge compartment at the base of lamellipodia.

To determine the approximate ratio of actin to tropomyosin at the leading edge, we quantified the fluorescence intensity for F-actin and tropomyosin as a percentage of the total fluorescence for each fluorophor in different regions of stimulated cells (Table 1). The greatest fraction of both actin and tropomyosin, and the highest actin-to-tropomyosin ratio, was in the stress fibers. If we assume actin filaments in stress fibers are saturated with tropomyosin, then by comparison of the fluorescence intensities, only ~25% of the filamentous actin at the leading edge [defined as the first 0.9 μm next to the membrane (Chan et al., 2000)] have tropomyosin bound. If the actin filaments in stress fibers are not saturated with tropomyosin, then 25% is an overestimate. In the base of lamellipodia (0.9-1.8 μm from the membrane), there is sufficient tropomyosin to saturate ~70% of the filamentous actin.

These calculations are based on the following measurements. In MTLn3 cells the total actin is about 153 mM (Edmonds et al., 1998), only about half of it being filamentous

Table 1. Fraction of F-actin and tropomyosin present in the leading edge, the base of the lamellipodium and stress fibers

	F-actin	Tropomyosin
Leading edge	9.0%	2.6%
Base of lamellipodium	7.6%	6.0%
Stress fibers	58.7%	65.7%

(Edmonds et al., 1996). Tropomyosin is 1.5-2% of the total protein, or ~25 mM [in chicken embryo fibroblasts and human blood platelets (Lin et al., 1985a) (S.E.H.-D., unpublished)], more than sufficient to saturate the filamentous actin with the usual 1 tropomyosin to 6 or 7 actin subunits in F-actin. When unstimulated MTLn3 cells growing in monolayers were permeabilized upon brief, mild, detergent treatment as in the experiments to assay barbed end labeling (see Materials and Methods), 15±4% (n=5) of the tropomyosin was extracted, based on quantitative analysis of tropomyosin using SDS-PAGE of supernatants and pellets. Similarly, analysis of immunofluorescence of cells stained for tropomyosin using the LC24 antibody showed an 18% loss of fluorescence intensity after saponin treatment of a monolayer of EGF stimulated cells (see Materials and Methods), presumably reflecting extraction of free tropomyosin not bound to actin. Assuming the extractable tropomyosin is unbound, there should be sufficient free tropomyosin (2.5-7.5 mM) to bind to F-actin with a K_d of 0.1 mM.

Tropomyosin is not associated with polymerizing filaments at the leading edge

The dynamic actin filament network at the leading edge was more specifically visualized by polymerizing biotin-labeled actin monomer into the barbed ends of growing actin filaments (Bailly et al., 1999; Chan et al., 1998). As previously reported (Bailly et al., 1999), unstimulated cells only had weak barbed-end staining at the leading edge (Fig. 3A), but cells EGF-stimulated for 50 seconds or 3 minutes showed an increase in the incorporation of actin monomer into filaments at the leading edge (Fig. 3F,K,P). The tropomyosin antibody αf9d stained actin stress fibers as well as more diffuse F-actin networks at the base of lamellipodia. However, αf9d did not label the dynamic leading edge compartment (Fig. 3B,G,L), which is enriched with barbed ends before and after EGF stimulation (see overlay in Fig. 3C,H,M). The CG3 antibody predominantly labeled perinuclear stress fibers but not the diffuse F-actin network at the base of lamellipodia [(Fig. 3Q) (Percival et al., 2000)] and did not colocalize with newly formed actin filaments at the leading edge (Fig. 3R). The difference in the staining patterns of the αf9d and CG3 antibodies with regard to the diffuse F-actin network at the base of lamellipodia is similar to that found in NIH 3T3 cells (Percival et al., 2000), suggesting these antibodies recognize different populations of microfilaments in MTLn3 cells as well. Fig. 3D,I,N,S show higher magnification images of the boxed areas in Fig. 3C,H,M,R. The tropomyosin staining (red)

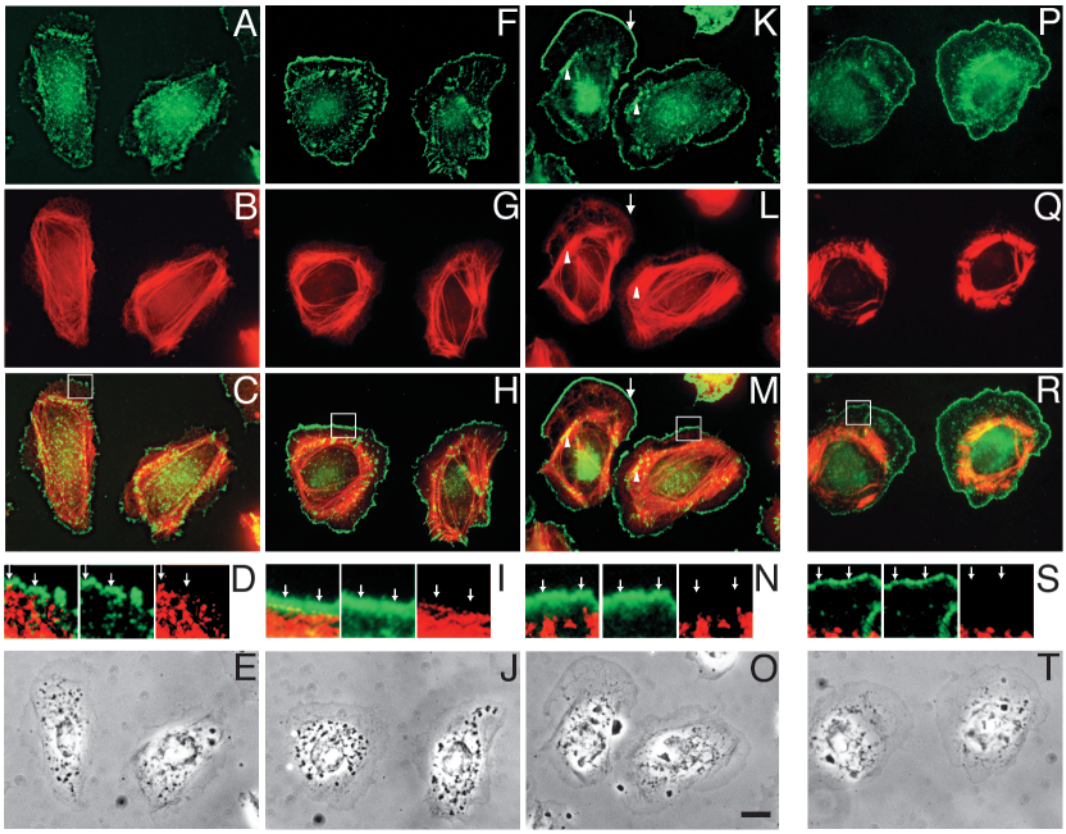

Fig. 3. Tropomyosin is not associated with the free barbed ends of growing actin filaments at the leading edge in resting and EGF-stimulated MTLn3 cells. Cells were either unstimulated (A-E), or stimulated with EGF for 50 seconds (F-J) or 3 minutes (K-T). Cells were double-labeled for barbed ends (A,F,K,P) and tropomyosin (αf9d,B,G,L; CG3,Q). Double-labeling overlays are shown (C,H,M,R; red, tropomyosin; green, barbed ends), as well as phase-contrast images (E,J,O,T). The white square in the overlay images (C,H,M,R) indicates an area that is shown at higher magnification directly below (D,I,N,S); from left to right: double labeling, barbed ends, tropomyosin. The size of the square is 7.5 μm by 7.5 μm. Bar, 10 μm. Arrows indicate regions at the leading edge with barbed ends, demonstrating the absence of tropomyosin. Arrowheads indicate regions of overlap between tropomyosin and barbed ends within stress fibers.

does not extend to the edge of the cell that is enriched in barbed ends of growing actin filaments (green).

Another probe for the dynamic actin filaments at the leading edge is the presence of the Arp2/3 complex. An antibody to the Arp2/3 complex, anti-p34, labeled the leading edge of the cells, especially after EGF stimulation (Fig. 4A,E,I) (Bailly et al., 1999). The tropomyosin antibody LC24 labeled stress fibers and actin networks within the cells, but did not label the leading edge at any time (Fig. 4B,F,J), as seen in the overlays (Fig. 4C,G,K). Similar results were obtained with antibody IV15 (Fig. 4N,O), which stained stress fibers as well as the base of lamellipodia, but not the leading edge compartment.

The localization of tropomyosin with respect to F-actin, free barbed ends and the Arp2/3 complex at the leading edge of lamellipodia is quantified in Fig. 5. The tropomyosin antibodies used in this analysis were LC24 and αf9d, which recognize many different tropomyosin isoforms, as discussed earlier. As described in the Materials and Methods, all measurements were in the linear range and above the noise level of the CCD camera. In unstimulated cells, tropomyosin was minimally associated with actin-containing structures close to the membrane, with the bulk of the labeling occurring much deeper in the cell as well as in stress fibers (Fig. 5A,D,G). Upon EGF stimulation, F-actin (phalloidin-actin), barbed end labeling and the Arp2/3 complex increased and peaked within 0.5 μm of the leading edge, but tropomyosin did not (Fig. 5B,C,E,F,H,I,J,K). Labeling for barbed ends and the Arp2/3 complex was maximal at 50 seconds of EGF stimulation, as previously reported [(Fig. 5D,E,F,G,H,I) (Bailly et al., 1999)]. The maximal labeling for F-actin, however, did not occur until 3 minutes of EGF stimulation (Fig. 5A,B,C,J). Tropomyosin remained minimal, possibly decreasing in amount at the edge (Fig. 5B,C,K). The localization of tropomyosin at the leading edge did not change upon EGF stimulation (Fig. 5K). This leading edge region is the same region of lamellipodia that contains branched actin filaments after EGF stimulation (Bailly et al., 1999).

Tropomyosin protects actin filaments from severing by cofilin

Previous biochemical results indicate that tropomyosin can inhibit the binding of cofilin to F-actin and cofilin-induced depolymerization (Bernstein and Bamburg, 1982; Nagaoka et al., 1995; Nishida et al., 1985; Ono and Ono, 2002). Since depolymerization and severing by cofilin are separable activities (Pope et al., 2000) and cofilin can sever actin filaments at concentrations 100-fold lower than that required for depolymerization (Ichetovkin et al., 2002), we tested the ability of tropomyosin to inhibit severing by cofilin using a light microscopy assay that directly measures the severing activity of cofilin (Fig. 6). Actin filaments were immobilized on nitrocellulose and addition of cofilin severed the actin filaments (Fig. 6, top panels). Pre-incubation of the actin filaments with TM5a, a short non-muscle isoform, inhibited cofilin's severing activity (Fig. 6, bottom panels).

Discussion

This study, as well as previous work (Bailly et al., 1999; Chan et al., 2000; Chan et al., 1998), demonstrates that there are several actin compartments within MTLn3 cells in which the actin filaments have different properties. These compartments differ with respect to the types of actin-associated proteins present. In the current study, we demonstrate that tropomyosin may have a role in establishing one of these actin compartments at the leading edge. Tropomyosin is relatively absent from the dynamic leading edge compartment, which

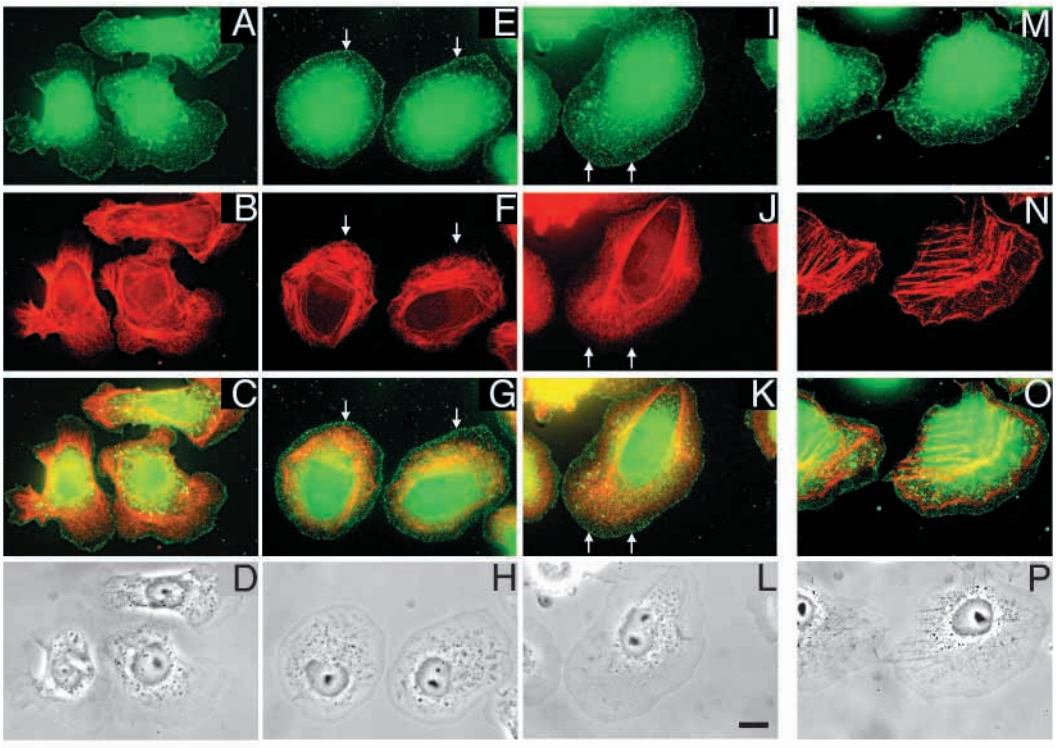

Fig. 4. Tropomyosin is absent from regions of the leading edge containing the Arp2/3 complex. Cells were either unstimulated (A-D), or stimulated with EGF for 50 seconds (E-H) or 3 minutes (I-P), and double-labeled for the Arp2/3 complex (anti-p34; A,E,I,M) and tropomyosin (LC24, B,F,J; IV15, N). Double-labeling overlays are shown in C, G, K and O (red, tropomyosin; green, the Arp2/3 complex). Phase contrast images are present in D, H, L and P. Bar, 10 μm. Arrows indicate regions at the leading edge where the Arp2/3 complex is localized demonstrating the absence of tropomyosin.

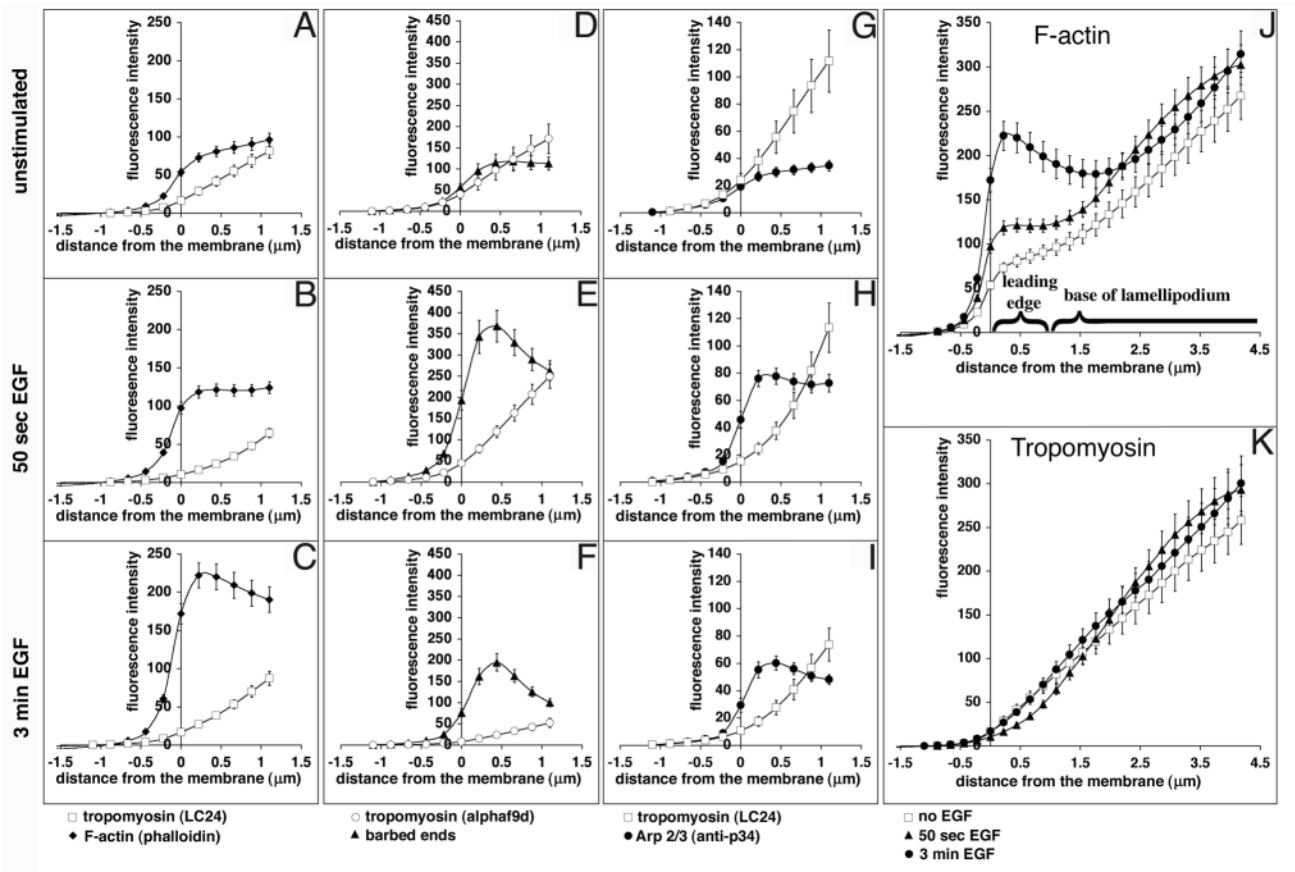

Fig. 5. Quantification of the relative locations of tropomyosin, F-actin, and the Arp2/3 complex at the leading edge. Cells analyzed were double-labeled for tropomyosin (LC24) and F-actin (rhodamine-phalloidin, A,B,C,J,K), tropomyosin (αf9d) and barbed ends (biotin-labeled G-actin, D,E,F), and tropomyosin (LC24) and the Arp2/3 complex (anti-p34, G,H,I) as in Figs 2-4. For panels A-I, cells were either unstimulated (A,D,G), or stimulated with EGF for 50 seconds (B,E,H) or 3 minutes (C,F,I). The fluorescence intensity (arbitrary units) is the mean of the cell perimeter in regions of the lamellipodium for 0.22 μm wide steps (see Materials and Methods). Quantification is shown within 1 μm of the cell membrane. After EGF stimulation, the F-actin, barbed ends and the Arp2/3 complex distribution peak within 0.5 μm of the membrane, while tropomyosin increases deeper in the lamellipodium. In panel J, quantification of F-actin is shown up to 4 μm beyond the cell membrane without EGF stimulation, 50 seconds and 3 minutes after EGF stimulation. Regions corresponding to the leading edge and the base of the lamellipodium are indicated. In panel K, quantification of tropomyosin (LC24) is shown up to 4 μm beyond the cell membrane without EGF stimulation, 50 seconds and 3 minutes after EGF stimulation. Error bars indicate standard error, with n=15 (A,B,C,J,K) and n=25 (D,E,F,G,H,I).

consists of the labile, branched actin network adjacent to the plasma membrane that is generated during rapid lamellipodium extension and is enriched in the Arp2/3 complex, barbed ends, and cofilin. However, tropomyosin is present in the stress fiber compartment and in actin networks in the base of lamellipodia (reviewed by Cooper, 2002).

We base our conclusion on negative immunofluorescence at the leading edge of protruding lamellipodia. One possible explanation for the absence of tropomyosin at the leading edge is that the tropomyosin epitopes are blocked in this region, which is unlikely, since none of the six antibodies we tested, that together detect all tropomyosin isoforms in MTLn3 cells, stained the leading edge, while they all stained actin structures elsewhere in the cell. It is improbable that the different epitopes recognized by the six antibodies would all be buried at the leading edge, but not in other cytoskeletal domains. The tropomyosin antibodies stained MTLn3 cells with similar intensity before and after EGF stimulation, suggesting that epitope availability does not correlate with protrusion or motility in this case. In addition, MTLn3 cells are continuously motile even before stimulation with EGF (Shestakova et al., 1999). This is unlike the case reported by Hegmann et al., where a correlation was found between motility and epitope availability for a monoclonal tropomyosin antibody (Hegmann et al., 1988).

The spatial segregation of tropomyosin isoforms in cells is well established (Gunning et al., 1998; Lin et al., 1988; Lin et al., 1997; Percival et al., 2000). Tropomyosin has long been known to be preferentially localized in regions of stable actin filaments in cells (Lazarides, 1976), but until now its distribution was not related to either actin function or other actin binding proteins in the actin-rich lamellipodium. Previous studies (Lin et al., 1988; Warren et al., 1985) showed the presence of tropomyosin in peripheral ruffles in normal chicken embryonic fibroblasts and transformed rat kidney cells. However, ruffles are structurally distinct from protruding lamellipodia observed in EGF stimulated MTLn3 cells. Protruding lamellipodia are planar with well-defined leading edges while ruffles are regions of membrane that fold back on themselves, are not planar and not necessarily regions of

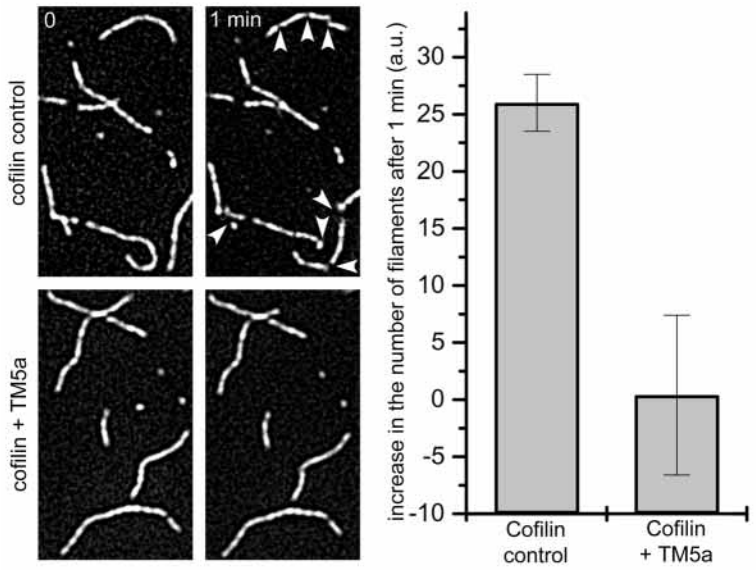

Fig. 6. Tropomyosin inhibits F-actin severing by cofilin. Rhodamine-biotin-labeled actin filaments were polymerized and attached to the surface of the perfusion chamber with anti-biotin antibody. Chambers were perfused with buffer or recombinant rat TM5a. All chambers were washed with cofilin storage buffer, and the first set of images was taken (time 0). Cofilin in the same buffer was perfused and 1 minute later another set of images was taken of the same field. Filaments saturated with TM5a did not show any severing while control filaments were severed by cofilin (arrowheads). While control fields show an increase in the number of filaments, pre-treatment of filaments with TM5a leads to the complete inhibition of this effect (right panel; a.u., arbitrary units).

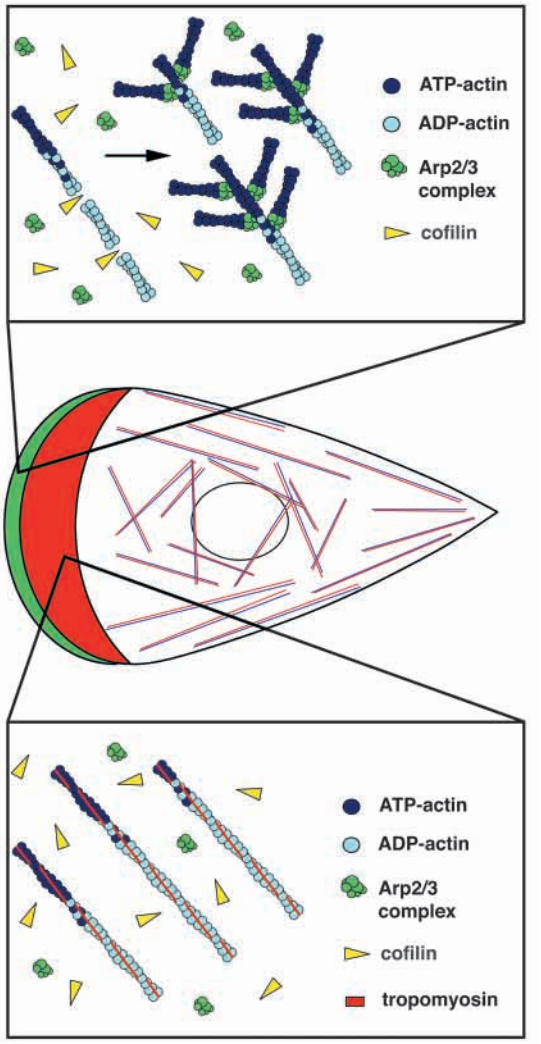

Fig. 7. Model of the actin compartments defined by tropomyosin in the cell. Three compartments are shown. Green, the dynamic leading edge compartment of the lamellipodium contains short actin filaments that are severed by cofilin. Here the Arp2/3 complex induces branch formation on newly polymerized actin filaments to give highly branched actin filaments (see top box). Tropomyosin is absent. Red: the second compartment is the base of the lamellipodium. It contains longer, unbranched actin filaments as well as tropomyosin bound to actin, free cofilin and free Arp2/3 complex. Tropomyosin stabilizes actin filaments and protects them from cofilin severing and Arp2/3 complex-induced branch formation (see bottom box). White: the third compartment is the main body of the cell that contains stress fibers stabilized by tropomyosin, as in the red compartment, and other actin binding proteins. The main body of the cell also contains free cofilin and Arp 2/3 complex.

outward extension but often retraction structures involved in endocytosis (Bailly et al., 1998b). Since MTLn3 cells cease to form ruffles during EGF stimulation and lamellipodia extension (Rotsch et al., 2001), the present study only focuses on whether tropomyosin is present in rapidly extending lamellipodia and their leading edges.

Fig. 7 is a model to illustrate three types of actin compartments defined by tropomyosin in protruding MTLn3 cells. The main body of the cell is rich in actin-containing structures, stress fibers and other long actin filaments containing tropomyosin that protects them from cofilin and other actin severing proteins, and prevents branch formation nucleated by the Arp2/3 complex. The lamellipodium of the cell is divided into two regions, the leading edge and base (Chan et al., 2000). In the base, the chronologically older region of the lamellipodium, there are long, unbranched actin filaments that contain tropomyosin, protected from cofilin and the Arp2/3 complex. Although cofilin and the Arp2/3 complex are distributed throughout the cell, a dynamic branched network of actin filaments forms only at the leading edge immediately under the plasma membrane (<1 μm) where tropomyosin is absent. Since the cofilin concentration is highest at the leading edge of carcinoma cells (Chan et al., 2000), cofilin mediated severing and depolymerization would occur at the leading edge and not at the base of lamellipodia, as has been proposed (Small et al., 2002).

The mechanism by which newly formed filaments of the leading edge are tropomyosin-poor remains to be established. Since the Arp2/3 complex and G-actin are rapidly recruited to the leading edge of lamellipodia upon stimulation, we would anticipate that tropomyosin would be too, if it could bind to the actin filaments there and if there are not dramatically different rates of diffusion. As mentioned in the Results section, there appears to be sufficient free tropomyosin (15-18%) in the cell to bind to F-actin. The low actin-to-tropomyosin ratio at the leading edge after stimulated protrusion (Table 1) during the peak period of cofilin and Arp2/3 complex activity over several minutes (Bailly et al.,

1999; Chan et al., 2000) suggests that something may prevent recruitment of tropomyosin to the leading edge filaments. Competitive inhibitors or a more direct regulation of binding of tropomyosin to newly formed actin filaments may exclude tropomyosin from the actin network

The demonstration that tropomyosin inhibits actin filament severing by cofilin is consistent with an antagonistic interaction between cofilin and tropomyosin that might confine the severing activity of cofilin to the leading edge actin filaments that are tropomyosin-free. Elevated concentrations of cofilin at the leading edge after EGF stimulation may inhibit binding of tropomyosin to F-actin. During stimulated protrusion of MTLn3 cells, cofilin is strongly recruited to the leading edge with 8% of the cell's 6-25 μM cofilin accumulating there at times of peak barbed end generation (Chan et al., 2000). Cofilin severs actin filaments at the leading edge, aiding in the nucleation of polymerization (Chan et al., 2000; Zebda et al., 2000). The high cofilin concentration relative to tropomyosin at the leading edge should be sufficient to competitively inhibit binding of tropomyosin to F-actin, possibly through changing the helical twist of the filament. Therefore, the timing of cofilin recruitment and activation at the leading edge by 50 seconds after stimulation (Chan et al., 2000) may prevent tropomyosin recruitment there. In the rest of the cell, much of the cofilin is likely to be inactivated by Lim kinase and less favorable pH (reviewed by Bamburg, 1999). The higher levels of tropomyosin would be able to protect actin filaments from severing by competing with any remaining active cofilin.

It is more difficult to evaluate the possible effect of the Arp2/3 complex on the distribution of tropomyosin at the leading edge. The Arp2/3 complex is approximately 2 μM in crawling cells (Bailly et al., 1999) and 3% is found in the leading edge in MTLn3 cells during the first 3 minutes of stimulated protrusion. There may be sufficient free tropomyosin to inhibit Arp2/3 complex nucleation and branching, based on in vitro experiments (Blanchoin et al., 2001), but few actin filaments have bound tropomyosin. However, little is known about the mechanism of Arp2/3 complex inhibition by tropomyosin. Also, only a small amount of this Arp2/3 complex will be active in the leading edge at any time. The complex moves away from the membrane quickly during protrusion (Bailly et al., 1999) as the Arp2/3 complex disassociates from the side of F-actin and WASp under the regulation of rapid nucleotide hydrolysis (Blanchoin et al., 2000b; Dayel et al., 2001). Nevertheless, any active Arp2/3 complex that does diffuse into a region where actin filaments have tropomyosin bound, such as the base of the lamellipodium, should be inhibited from nucleation and branching.

Recent work is consistent with synergy between the Arp2/3 complex and cofilin in the formation of a dynamic, branched actin filament network at the leading edge (Ichetovkin et al., 2002). The Arp2/3 complex-mediated branch formation in vitro preferentially occurs from the sides of newly grown filaments containing ATP-actin. Since the dynamic leading edge compartment contains branched, rapidly polymerizing actin networks, it is likely that filaments in this region are enriched in ATP-actin near the fast growing ends (ATP caps). This would bias the Arp2/3 complex-generated branched filaments to grow in one direction, the direction of lamellipodium extension. Thus, it appears that the Arp2/3 complex binds to and initiates branching of newly polymerized actin filaments at the leading edge, while tropomyosin protects older, ADP-actin containing filaments away from the leading edge from the binding and activation of the Arp2/3 complex.

The leading edge of cells may also be the site of other functions inhibited by tropomyosin. Tang and Ostap reported that myosin 1b, a myosin whose motile function is inhibited by tropomyosin, is localized in the tropomyosin-poor, actin-rich cortex of NRK cells that would be expected to contain the Arp2/3 complex (Tang and Ostap, 2001).

The results presented here, as well as previously published work, may explain how cofilin severing and the Arp2/3 complex-nucleated branching result in new filament ends and filament branching only at the leading edge even though both proteins are present throughout the cytoplasm. Only filaments not saturated with tropomyosin are severed upon activation of cofilin or serve as substrates for branch formation. Therefore, even if cofilin and the Arp2/3 complex were globally activated, they would only act on filaments free of tropomyosin, such as those at the leading edge.

We are grateful to Peter Gunning, Jim Lin and Fumio Matsumura for generously providing antibodies to tropomyosin. We thank Maryse Bailly for introducing us to the techniques used for the cellular studies, Yuhua Song and Sarah Graboski for assistance in quantification of tropomyosin in cell extracts, and Michael Cammer for assistance in image analysis. This research was supported by NIH HL35726/63257 to S.E.H.-D. and grants from the NIH to J.C.

References

Agnew, B. J., Minamide, L. S. and Bamburg, J. R. (1995). Reactivation of phosphorylated actin depolymerizing factor and identification of the regulatory site. *J. Biol. Chem.* **270**, 17582-17587.

Bailly, M., Condeelis, J. S. and Segall, J. E. (1998a). Chemoattractant-induced lamellipod extension. *Microsc. Res. Tec.* **43**, 433-443.

Bailly, M., Yan, L., Whitesides, G. M., Condeelis, J. S. and Segall, J. E. (1998b). Regulation of protrusion shape and adhesion to the substratum during chemotactic responses of mammalian carcinoma cells. *Exp. Cell Res.* **241**, 285-299.

Bailly, M., Macaluso, F., Cammer, M., Chan, A., Segall, J. E. and Condeelis, J. S. (1999). Relationship between Arp2/3 complex and the barbed ends of actin filaments at the leading edge of carcinoma cells after epidermal growth factor stimulation. *J. Cell Biol.* **145**, 331-345.

Bailly, M., Ichetovkin, I., Grant, W., Zebda, N., Machesky, L. M., Segall, J. E. and Condeelis, J. (2001). The F-actin side binding activity of the Arp2/3 complex is essential for actin nucleation and lamellipod extension. *Curr. Biol.* **11**, 620-625.

Bamburg, J. R. (1999). Proteins of the ADF/cofilin family: essential regulators of actin dynamics. *Annu. Rev. Cell Dev. Biol.* **15**, 185-230.

Bamburg, J. R., Minamide, L. S., Morgan, T. E., Hayden, S. M., Giuliano, K. A. and Koffer, A. (1991). Purification and characterization of low-molecular-weight actin-depolymerizing proteins from brain and cultured cells. *Methods Enzymol.* **196**, 125-140.

Bernstein, B. W. and Bamburg, J. R. (1982). Tropomyosin binding to F-actin protects the F-actin from disassembly by brain actin-depolymerizing factor (ADF). *Cell Motil.* **2**, 1-8.

Blanchoin, L., Amann, K. J., Higgs, H. N., Marchand, J. B., Kaiser, D. A. and Pollard, T. D. (2000a). Direct observation of dendritic actin filament networks nucleated by Arp2/3 complex and WASP/Scar proteins. *Nature* **404**, 1007-1011.

Blanchoin, L., Pollard, T. D. and Mullins, R. D. (2000b). Interactions of ADF/cofilin, Arp2/3 complex, capping protein and profilin in remodeling of branched actin filament networks. *Curr. Biol.* **10**, 1273-1282.

Blanchoin, L., Robinson, R. C., Choe, S. and Pollard, T. D. (2000c). Phosphorylation of Acanthamoeba actophorin (ADF/cofilin) blocks interaction with actin without a change in atomic structure. *J. Mol. Biol.* **295**, 203-211.

Blanchoin, L., Pollard, T. D. and Hitchcock-DeGregori, S. E. (2001).

Inhibition of the Arp2/3 complex-nucleated actin polymerization and branch formation by tropomyosin. *Curr. Biol.* **11**, 1300-1304.
Borisy, G. G. and Svitkina, T. M. (2000). Actin machinery: pushing the envelope. *Curr. Opin. Cell. Biol.* **12**, 104-112.
Carlier, M. F., Laurent, V., Santolini, J., Melki, R., Didry, D., Xia, G. X., Hong, Y., Chua, N. H. and Pantaloni, D. (1997). Actin depolymerizing factor (ADF/cofilin) enhances the rate of filament turnover: implication in actin-based motility. *J. Cell Biol.* **136**, 1307-1322.
Chan, A. Y., Raft, S., Bailly, M., Wyckoff, J. B., Segall, J. E. and Condeelis, J. S. (1998). EGF stimulates an increase in actin nucleation and filament number at the leading edge of the lamellipod in mammary adenocarcinoma cells. *J. Cell Sci.* **111**, 199-211.
Chan, A. Y., Bailly, M., Zebda, N., Segall, J. E. and Condeelis, J. S. (2000). Role of cofilin in epidermal growth factor-stimulated actin polymerization and lamellipod protrusion. *J. Cell Biol.* **148**, 531-542.
Condeelis, J. (2001). How is actin polymerization nucleated in vivo? *Trends Cell. Biol.* **11**, 288-293.
Cooper, J. A. (2002). Actin dynamics: tropomyosin provides stability. *Curr. Biol.* **12**, R523-R525.
Cramer, L. P. (1999). Role of actin-filament disassembly in lamellipodium protrusion in motile cells revealed using the drug jasplakinolide. *Curr. Biol.* **9**, 1095-1105.
Dayel, M. J., Holleran, E. A. and Mullins, R. D. (2001). Arp2/3 complex requires hydrolyzable ATP for nucleation of new actin filaments. *Proc. Natl. Acad. Sci. USA* **98**, 14871-14876.
Edmonds, B. T., Wyckoff, J., Yeung, Y. G., Wang, Y., Stanley, E. R., Jones, J., Segall, J. and Condeelis, J. (1996). Elongation factor-1 alpha is an overexpressed actin binding protein in metastatic rat mammary adenocarcinoma. *J. Cell Sci.* **109**, 2705-2714.
Edmonds, B. T., Bell, A., Wyckoff, J., Condeelis, J. and Leyh, T. S. (1998). The effect of F-actin on the binding and hydrolysis of guanine nucleotide by Dictyostelium elongation factor 1A. *J. Biol. Chem.* **273**, 10288-10295.
Gunning, P., Hardeman, E., Jeffrey, P. and Weinberger, R. (1998). Creating intracellular structural domains: spatial segregation of actin and tropomyosin isoforms in neurons. *Bioessays* **20**, 892-900.
Hawkins, M., Pope, B., Maciver, S. K. and Weeds, A. G. (1993). Human actin depolymerizing factor mediates a pH-sensitive destruction of actin filaments. *Biochemistry* **32**, 9985-9993.
Hegmann, T. E., Lin, J. L. and Lin, J. J. (1988). Motility-dependence of the heterogenous staining of culture cells by a monoclonal anti-tropomyosin antibody. *J. Cell Biol.* **106**, 385-393.
Higgs, H. N. and Pollard, T. D. (2001). Regulation of actin filament network formation through Arp2/3 complex: activation by a diverse array of proteins. *Annu. Rev. Biochem.* **70**, 649-676.
Ichetovkin, I., Han, J., Pang, K. M., Knecht, D. A. and Condeelis, J. S. (2000). Actin filaments are severed by both native and recombinant dictyostelium cofilin but to different extents. *Cell Motil. Cytoskeleton* **45**, 293-306.
Ichetovkin, I., Grant, W. and Condeelis, J. S. (2002). Cofilin produces newly polymerized actin filaments that are preferred for dendritic nucleation by the Arp2/3 complex. *Curr. Biol.* **12**, 1-20.
Lauffenburger, D. and Horwitz, A. (1996). Cell migration: a physically integrated molecular process. *Cell* **84**, 359-369.
Lazarides, E. (1976). Two general classes of cytoplasmic actin filaments in tissue culture cells: the role of tropomyosin. *J. Supramol. Struct.* **5**, 531(383)-563(415).
Lin, J. J., Chou, C. S. and Lin, J. L. (1985a). Monoclonal antibodies against chicken tropomyosin isoforms: production, characterization, and application. *Hybridoma* **4**, 223-242.
Lin, J. J., Helfmann, D. M., Hughes, S. H. and Chou, C. S. (1985b). Tropomyosin isoforms in chicken embryo fibroblasts: purification, characterization, and changes in Rous sarcoma virus-transformed cells. *J. Cell Biol.* **100**, 692-703.
Lin, J. J., Hegmann, T. E. and Lin, J. L. (1988). Differential localization of tropomyosin isoforms in cultured nonmuscle cells. *J. Cell Biol.* **107**, 563-572.
Lin, J. J., Warren, K. S., Wamboldt, D. D., Wang, T. and Lin, J. L. (1997). Tropomyosin isoforms in nonmuscle cells. *Int. Rev. Cytol.* **170**, 1-38.
Matsumura, F., Yamashiro-Matsumura, S. and Lin, J. J. (1983). Isolation and characterization of tropomyosin-containing microfilaments from cultured cells. *J. Biol. Chem.* **258**, 6636-6644.
Moraczewska, J., Nicholson-Flynn, K. and Hitchcock-DeGregori, S. E. (1999). The ends of tropomyosin are major determinants of actin affinity and myosin subfragment 1-induced binding to F-actin in the open state. *Biochemistry* **38**, 15885-15892.
Moriyama, K., Iida, K. and Yahara, I. (1996). Phosphorylation of Ser-3 of cofilin regulates its essential function on actin. *Genes Cells* **1**, 73-86.
Mullins, R. D., Heuser, J. A. and Pollard, T. D. (1998). The interaction of Arp2/3 complex with actin: nucleation, high affinity pointed end capping, and formation of branching networks of filaments. *Proc. Natl. Acad. Sci. USA* **95**, 6181-6186.
Nagaoka, R., Kusano, K., Abe, H. and Obinata, T. (1995). Effects of cofilin on actin filamentous structures in cultured muscle cells. Intracellular regulation of cofilin action. *J. Cell Sci.* **108**, 581-593.
Nicholson-Flynn, K., Hitchcock-DeGregori, S. E. and Levitt, P. (1996). Restricted expression of the actin-regulatory protein, tropomyosin, defines distinct boundaries, evaginating neuroepithelium, and choroid plexus forerunners during early CNS development. *J. Neurosci.* **16**, 6853-6863.
Nishida, E., Muneyuki, E., Maekawa, S., Ohta, Y. and Sakai, H. (1985). An actin-depolymerizing protein (destrin) from porcine kidney. Its action on F-actin containing or lacking tropomyosin. *Biochemistry* **24**, 6624-6630.
Ono, S. and Ono, K. (2002). Tropomyosin inhibits ADF/cofilin-dependent actin filament dynamics. *J. Cell Biol.* **156**, 1065-1076.
Percival, J. M., Thomas, G., Cock, T. A., Gardiner, E. M., Jeffrey, P. L., Lin, J. J., Weinberger, R. P. and Gunning, P. (2000). Sorting of tropomyosin isoforms in synchronised NIH 3T3 fibroblasts: evidence for distinct microfilament populations. *Cell Motil. Cytoskeleton* **47**, 189-208.
Pollard, T. D., Blanchoin, L. and Mullins, R. D. (2000). Molecular mechanisms controlling actin filament dynamics in nonmuscle cells. *Annu. Rev. Biophys. Biomol. Struct.* **29**, 545-576.
Pope, B. J., Gonsior, S. M., Yeoh, S., McGough, A. and Weeds, A. G. (2000). Uncoupling actin filament fragmentation by cofilin from increased subunit turnover. *J. Mol. Biol.* **298**, 649-661.
Ressad, F., Didry, D., Xia, G. X., Hong, Y., Chua, N. H., Pantaloni, D. and Carlier, M. F. (1998). Kinetic analysis of the interaction of actin-depolymerizing factor (ADF)/cofilin with G- and F-actins. Comparison of plant and human ADFs and effect of phosphorylation. *J. Biol. Chem.* **273**, 20894-20902.
Rotsch, C., Jacobson, K., Condeelis, J. and Radmacher, M. (2001). EGF-stimulated lamellipod extension in adenocarcinoma cells. *Ultramicroscopy* **86**, 97-106.
Schevzov, G., Gunning, P., Jeffrey, P. L., Temm-Grove, C., Helfman, D. M., Lin, J. J. and Weinberger, R. P. (1997). Tropomyosin localization reveals distinct populations of microfilaments in neurites and growth cones. *Mol. Cell Neurosci.* **8**, 439-454.
Segall, J. E., Tyerech, S., Boselli, L., Masseling, S., Helft, J., Chan, A., Jones, J. and Condeelis, J. (1996). EGF stimulates lamellipod extension in metastatic mammary adenocarcinoma cells by an actin-dependent mechanism. *Clin. Exp. Metastasis* **14**, 61-72.
Shestakova, E. A., Wykoff, J., Jones, J., Singer, S. H. and Condeelis, J. (1999). Correlation of beta-actin messenger RNA localization with metastatic potential in rat adenocarcinoma cell lines. *Cancer Res.* **59**, 1202-1205.
Small, J. V., Isenberg, G. and Celis, J. E. (1978). Polarity of actin at the leading edge of cultured cells. *Nature* **272**, 638-639.
Small, J. V., Herzog, M. and Anderson, K. (1995). Actin filament organization in the fish keratocyte lamellipodium. *J. Cell Biol.* **129**, 1275-1286.
Small, J. V., Stradal, T., Vignal, E. and Rottner, K. (2002). The lamellipodium: where motility begins. *Trends Cell Biol* **12**, 112-120.
Spudich, J. A. and Watt, S. (1971). The regulation of rabbit skeletal muscle contraction. I. Biochemical studies of the interaction of the tropomyosin-troponin complex with actin and the proteolytic fragments of myosin. *J. Biol. Chem.* **246**, 4866-4871.
Svitkina, T. M. and Borisy, G. G. (1999). Arp2/3 complex and actin depolymerizing factor/cofilin in dendritic organization and treadmilling of actin filament array in lamellipodia. *J. Cell Biol.* **145**, 1009-1026.
Tang, N. and Ostap, E. M. (2001). Motor domain-dependent localization of myo1b (myr-1). *Curr. Biol.* **11**, 1131-1135.
Uruno, T., Liu, J., Zhang, P., Fan, Y., Egile, C., Li, R., Mueller, S. C. and Zhan, X. (2001). Activation of Arp2/3 complex-mediated actin polymerization by cortactin. *Nat. Cell Biol.* **3**, 259-266.
Vera, C., Sood, A., Gao, K. M., Yee, L. J., Lin, J. J. and Sung, L. A. (2000). Tropomodulin-binding site mapped to residues 7-14 at the N-terminal heptad repeats of tropomyosin isoform 5. *Arch. Biochem. Biophys.* **378**, 16-24.

Warren, R. H., Gordon, E. and Azarnia, R. (1985). Tropomyosin in peripheral ruffles of cultured rat kidney cells. *Eur. J. Cell Biol.* **38**, 245-253.

Weaver, A. M., Karginov, A. V., Kinley, A. W., Weed, S. A., Li, Y., Parsons, J. T. and Cooper, J. A. (2001). Cortactin promotes and stabilizes Arp2/3-induced actin filament network formation. *Curr. Biol.* **11**, 370-374.

Weber, A., Pennise, C. R., Babcock, G. G. and Fowler, V. M. (1994). Tropomodulin caps the pointed ends of actin filaments. *J. Cell Biol.* **127**, 1627-1635.

Weber, A., Pennise, C. R. and Fowler, V. M. (1999). Tropomodulin increases the critical concentration of barbed end-capping actin filaments by converting ADP.P(i)-actin to ADP-actin at all pointed filament ends. *J. Biol. Chem.* **274**, 34637-34645.

Zebda, N., Bernard, O., Bailly, M., Welti, S., Lawrence, D. S. and Condeelis, J. S. (2000). Phosphorylation of ADF/cofilin abolishes EGF-induced actin nucleation at the leading edge and subsequent lamellipod extension. *J. Cell Biol.* **151**, 1119-1128.